

REVIEW

Nanostructured thin films of degradable block copolymers and their applications

Ming-Shiuan She, Ting-Ya Lo, Han-Yu Hsueh and Rong-Ming Ho

Nanopatterning using self-assembled thin films of degradable block copolymers (BCPs) has attracted considerable attention and inspired a variety of appealing applications in different research areas. To create useful nanopatterns for practical uses, controlling the orientation of the BCP microdomains is essential. The generation of oriented microdomains in BCP thin films will be discussed in this article. This discussion is followed by a review of methods that use polylactide-containing BCP (that is, polystyrene-*b*-poly(L-lactide) (PS-PLLA)) thin films to generate nanoporous PS after hydrolysis, which can be used for templated synthesis to create functional nanohybrids. The nanoporous PS thin films with well-oriented cylinder nanochannels can be used for pore-filling various ingredients to create specific drug delivery systems and optoelectronic devices. Moreover, by utilizing templated synthesis, nanoporous ceramics with a high-specific surface area and high porosity can be fabricated for optical applications using hydrolyzed gyroid-forming PS-PLLA as a template for the sol-gel reaction. In addition, the nanolithography applications using silicon-containing BCP (that is, polystyrene-*b*-polydimethylsiloxane) thin films, which can form inorganic nanoporous templates after oxygen plasma treatment, will be discussed in this review.

NPG Asia Materials (2013) 5, e42; doi:10.1038/am.2013.5; published online 15 March 2013

Keywords: block copolymers; nanopattern; orientation; thin films

In recent decades, block copolymers (BCPs) have been extensively investigated because of their ability to self-assemble into various ordered nanostructures, such as spheres, cylinders, gyroids and lamellae, owing to the incompatibility of their constituent blocks and the corresponding chemical junction.^{1,2} Well-defined nanostructured phases can be tailored by the molecular engineering of synthetic BCPs to obtain promising features for nanotechnological applications. For such nanostructured materials to prove useful in thin-film applications, thin-film samples with oriented periodic arrays over a large area must be formed to generate a uniform thickness and sufficiently thin films with well-ordered BCP microdomains. Nanoporous materials from BCP thin films have been attracted considerable attention owing to their appealing applications in different research areas. The etching techniques used to generate nanoporous materials can be classified as wet and dry processes depending on the etching methods.³ The wet etching process is a common approach for fabricating nanoporous materials. By utilizing the degradable character of polymer chains, nanoporous polymers can be fabricated using self-assembled nanostructures through the selective degeneration of one of the constituent blocks. For instance, polylactide-containing BCPs can be used to fabricate nanoporous polymeric materials because of the unstable character of the ester group, which can be hydrolytically decomposed.⁴ After hydrolysis of the polylactide segments, a nanoporous thin film with a uniform thickness and domain size can be successfully prepared on different

substrates. Consequently, the nanoporous thin films can be used as nanoreactors to fabricate functional nanomaterials for electronic, optical and biomedical applications. In contrast, the dry etching processes are conducted in vacuum, and the removable component will decompose under exposure to the electron or plasma ion. For instance, silicon-containing BCPs (such as polystyrene-*b*-polydimethylsiloxane (PS-PDMS)) can be used to fabricate nanoporous materials by plasma ion etching because of the high density of Si in the backbone of the BCP, which provides an extremely high etching contrast between the constituent blocks under oxygen plasma treatment.⁵ By utilizing the extremely high etching contrast, silicon-containing BCP thin films can be used as masks for pattern transfer in nanolithography applications.⁶

In this review, the generation of oriented microdomains in degradable BCP thin films, specifically polystyrene-*b*-poly(L-lactide) (PS-PLLA) thin films, will be discussed. By utilizing the hydrolytic treatment (a wet etching process), nanoporous templates can be generated from self-assembled PS-PLLA that can be used for templated-syntheses to create functional nanohybrids. The nanoporous PS thin films with well-oriented cylinder nanochannels can be used for pore-filling with various ingredients to create specific drug delivery systems and optoelectronic devices. Moreover, by utilizing templated-syntheses, nanoporous ceramics with high-specific surface areas and high porosities can be fabricated for optical applications using hydrolyzed gyroid-forming PS-PLLA as a template for the sol-

gel reaction. In addition, the formation of inorganic nanoporous templates from self-assembled PS-PDMS after oxygen plasma treatment (a dry etching process) and its corresponding applications in nanolithography will be discussed.

ORIENTATION OF BCP THIN FILMS

Solvent-induced orientation of cylindrical nanostructures in BCP thin films

Many applications that use BCP thin films as templates or scaffolds only require the orientation of the microdomains to be normal to the cylinder-forming nanostructured thin films. Accordingly, different approaches for controlling the orientation of microphase-separated nanostructures from self-assembled BCP have been developed. These approaches include solvent evaporation,^{7–10} solvent annealing,^{11–15} the application of shear fields,^{16–20} the application of electric fields,^{21–23} the use of temperature gradients,^{24,25} epitaxial crystallization,^{26–28} chemical patterning of the surface^{29–33} and graphoepitaxy.^{34–38} Solvent field (that is, solvent evaporation or solvent annealing) has proven to be a very simple, yet highly effective, method to manipulate the orientation and lateral ordering of BCP microdomains. Libera and co-workers⁷ were the first to demonstrate the effect of solvent evaporation on the orientation of cylindrical microdomains normal to the film surface in a range of different BCP thin films. Slow solvent extraction rates lead to a parallel alignment of the cylindrical microdomains in BCP thin films. Upon fast drying, a perpendicular orientation of the cylinders can be observed.⁹ In our previous studies, the preparation of perpendicular PLLA cylinders in the PS-PLLA thin film was achieved by controlling the evaporation rate of the solvent and the selectivity of the solvent with constituent blocks of the PS-PLLA.³⁹ The mechanism for the morphological evolution of microphase separation is proposed as shown in Figure 1. The microphase separation is initiated from the air surface at which the formed morphology adopts a perpendicular orientation due to permeation considerations, in particular the permeation of solvent to the surface. Following the nucleation of microphase separation, the solvent molecules are evaporated through the higher permeation microdomains to create a solvent concentration gradient within the film. The development of a perpendicular morphology continuously proceeds from the free surface owing to the epitaxy-like growth through the entire film. The solvent concentration gradient will be subtle under conditions in which the solvent is allowed to evaporate relatively fast. Eventually, the straight

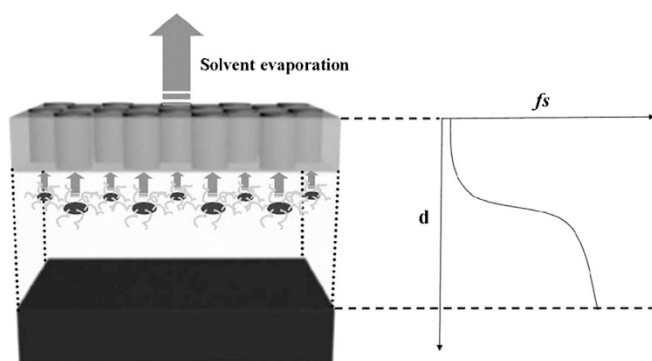


Figure 1 The schematic illustration for the formation of a PS-PLLA nanopattern prepared by spin-coating, which is similar to the mechanism proposed by Kim and co-workers⁷, in which f_s is the volume fraction of solvent and d is the depth of the thin film.³⁹

perpendicular cylinders in the films are formed from the top to the bottom in the direction of the maximum solvent concentration gradient. Note that a thin PLLA layer might be formed under conditions with a low evaporation rate, particularly at hydrophilic substrates. Accordingly, casting was performed at a temperature above the glass transition temperature of PLLA in which the evaporation rate can be sufficiently fast to lead the kinetically controlled process to avoid the formation of a thin PLLA layer. Consequently, the cylindrical PLLA nanostructures can span through the entire thickness of the film.

Well-ordered gyroid nanostructures in BCP thin films under solvent vapor

In addition to controlling the orientation of cylindrical nanostructures, the long-range order of the cylindrical nanostructures in thin films of BCPs can also be important for applications that require addressability. Uncontrolled processes usually give rise to locally well-defined nanostructures, but grains of the microdomains are small and randomly arranged on the surface. Among the several plausible routes to enhance the lateral order in thin films of BCPs, annealing in solvent vapors has been shown to be effective in enhancing the lateral order over very large areas.^{11–15} For instance, Russell and co-workers^{11,13} have investigated the thin-film morphologies of polystyrene-*b*-poly(ethylene oxide) (PS-PEO) and polystyrene-*b*-poly(4-vinylpyridine) (PS-P4VP) after annealing in solvent vapors for different amounts of time. With increasing annealing time, the lateral ordering of the cylindrical nanostructures can be significantly increased. Consequently, BCP thin films with a hexagonal ordering of the cylindrical nanostructures can be achieved by vapor annealing. Furthermore, gyroid nanostructures formed from the self-assembly of BCPs can be achieved by solvent annealing. Abetz and co-workers⁴⁰ have investigated the thin-film morphologies of polystyrene-*b*-poly(2-vinylpyridine) (PS-P2VP) diblock copolymers and polystyrene-*b*-poly(2-vinylpyridine)-*b*-poly(*tert*-butyl methacrylate) triblock copolymers after annealing in the vapors of different solvents. A core-shell double gyroid aligned with the surface parallel to its (211) plane in the polystyrene-*b*-poly(2-vinylpyridine)-*b*-poly(*tert*-butyl methacrylate) films can be observed after annealing in chloroform vapor. Recently, we demonstrated the fabrication of well-defined gyroid nanostructures with controlled thicknesses of ~ 150 nm.^{41,42} A spin-coating process for the preparation of PS-PLLA thin films was first conducted to create thin films with a uniform thickness. Subsequently, the solvent-annealing process was conducted to acquire the equilibrium morphology as a gyroid nanostructure with a large-scale orientation. The thin-film morphologies are different than the morphology of the bulk sample when the thickness of the PS-PLLA thin films is approximately four-times smaller than the *d*-spacing of the (211) plane. Consequently, the equilibrium morphology can be obtained as a gyroid nanostructure.

Nanoporous thin-film templates from degradable BCPs

The fabrication of nanoporous materials is of interest for applications. Because the pore size of nanoporous thin films and the corresponding separation distance between the pores can be varied with the use of BCPs, they have received considerable attention for use as templates or scaffolds for fabricating nanostructured materials. The typical methods for generating nanoporous materials from the self-assembly of BCPs can be classified as wet and dry processes. The hydrolysis of polylactide, ozonolysis of polybutadiene and polyisoprene and the UV degradation of polymethylmethacrylate (PMMA) are examples of wet approaches in which the BCP must interact with a specific reagent to

cause degradation of the sacrificial block.^{4,39,43–52} Polylactide-containing BCPs (such as polystyrene-*b*-poly(D,L-lactide) (PS-PLA) and PS-PLLA) are highly suited for the fabrication of nanoporous polymers because of the unstable character of the ester group, which can be hydrolytically decomposed. Consequently, chemically degradable BCPs have attracted considerable attention for use in nanofabrication. A successful method for the hydrolysis of PLA in the PS-PLA bulk state has been demonstrated by Hillmyer and co-workers.⁴ A 0.5 M solution was prepared by dissolving sodium hydroxide in a 40:60 v/v% solution of methanol and water. The hydrolysis was performed by placing a PS-PLA sample in the aqueous methanol solution at 65 °C. After the hydrolytic process, the sample was washed with water and methanol and then it was dried under vacuum at room temperature. Following the successful procedure for the hydrolysis of PLA, perpendicular cylindrical nanochannels in PS-PLLA thin films can be simply obtained by hydrolysis, as evidenced by field-emission scanning electron microscopy (FESEM) images (Figure 2a).³⁹ Furthermore, the cylindrical nanochannels in the hydrolyzed nanopatterns are actually spanned through the entire thickness of the films, as evidenced by the cross-sectional view in the FESEM image (Figure 2b).

NANOHYBRIDS FROM NANOPOROUS THIN-FILM TEMPLATES AND THEIR APPLICATIONS

Capillary forces for pore-filling process

For many complex devices in the applications of nanotechnology, it is preferable to assemble semiconductors, metals or inorganic particles into nanostructures through templating; therefore, the pore-filling process for nanoporous materials has been extensively exploited for the fabrication of nanohybrid materials. Nanoporous thin-film templates generated by scarifying one of the constituent blocks can consequently serve as templates for fabricating nanohybrid materials using the pore-filling process. Various approaches for filling functional materials into the pores of BCP thin-film templates have already been demonstrated. Capillary force, which is also called capillary attraction or capillarity, is used to pore-fill the ingredients into the pores. Russell and co-workers⁵³ demonstrated a directed deposition method by introducing nanoparticles into the cylindrical nanochannels of BCP films through the pore-filling process using directed capillary force. To further examine the features in the pore-filling process with nanoparticles in BCP thin-film templates, various pore-filling processes have been investigated in our laboratory (Figure 3).⁵⁴ Note that the pore-filling process involves the thrust of capillary force driven from the tunable wetting property of the solution for the templates. Accordingly, methanol is used to promote

the wetting tendency of the solution of cadmium ions into the PS template through capillary rise. Furthermore, water is introduced into the methanol solution to enhance the surface tension for the deposition of the thin-film template that is uniformly floating on the surface of solution, whereas the solution can still wet the PS template by appropriately adjusting the ratio of methanol and water as a mixed solvent. Consequently, CdS nanocrystals were generated *in-situ* by exposing the template incorporated with cadmium acetate to H₂S vapor after the pore-filling process.

Furthermore, an immunosuppressive agent with anti-inflammation and anti-proliferation characteristics, sirolimus, was also pore-filled into the PS template to provide better control over the release of the drug.⁵⁵ As mentioned above, the wetting property is critical for achieving a successful pore-filling process by directed capillary force. To increase the wetting ability of the capillary force, a solution of sirolimus was prepared by dissolving it in a mixed solvent of ethanol and water. Consequently, sirolimus was successfully introduced into the oriented cylindrical nanochannels via the pore-filling process. Figure 4 presents the results of *in vitro* drug elution from the sirolimus-loaded cylindrical nanoarrays; the nanoarrays obtained from the anodized aluminum oxide (AAO)/sirolimus hybrids and the PS/sirolimus blends were used as controls. The release profiles from the AAO/sirolimus hybrids and the PS/sirolimus blends reveal a rapid release of the drug with an initial burst releasing effect. In contrast, the drug-release profile observed from the sirolimus-loaded cylindrical nanoarrays exhibits no burst release; instead, a prolonged and sustained-release profile can be observed. Because the sirolimus-loaded cylindrical nanoarrays are made from the cylindrical nanochannels (20 nm in diameter), the sirolimus can be effectively entrapped, which results in a well-controlled, specific release profile.

Recently, we also demonstrated a simple method for generating ordered poly(2,3-diphenyl-5-(trimethylene-octa(oxyethylene)-methoxy)-phenylenevinylene) (DP-PPV-PEO)-conjugated polymer nanoarrays through a pore-filling process by solvent annealing.⁵⁶ The nanoporous PS template was removed from a glass substrate, floated on an aqueous surface and then finally collected by a glass substrate coated with the DP-PPV-PEO thin film. Subsequently, the nanoporous PS template on the spin-coated PVE thin film was treated with the solvent vapor of acetic acid at different accumulated annealing times. As shown in Figure 5a, the initial morphology reveals the surface of nanoporous PS template with a height difference of 8–11 nm at annealing time $t=0$. After the solvent-annealing treatment was performed for 24 h, the partially filled template reveals a decrease in the height difference to 2–4 nm. With further annealing to 48 h, the majority of the nanopores can be filled with the DP-PPV-PEO. After solvent annealing for 72 h, the PS surface is covered by the DP-PPV-PEO owing to the strong affinity between the PVE chain and acetic acid. The corresponding evolution of the photoluminescence spectra was monitored by measuring the luminescence. As shown in the insets of Figures 5b and c, the photoluminescence intensity of the DP-PPV-PEO peak increases with annealing time and then reaches a maximum at 48 h. With further annealing, the intensity of the DP-PPV-PEO peak significantly decreases. The enhanced luminescence is attributed to the increase of chain alignment in the PPV backbone driven by the nanoscale spatial effect for pore-filled DP-PPV-PEO. Once the DP-PPV-PEO releases from the nanopores through pore-filling after annealing for 72 h, the polymer chains in the wetting layer are randomized to cause a significant self-quenching problem. Consequently, the enhanced luminescence of DP-PPV-PEO nanostructure driven by the nanoscale spatial effect is highly promising for use in designing luminescent nanodevices.

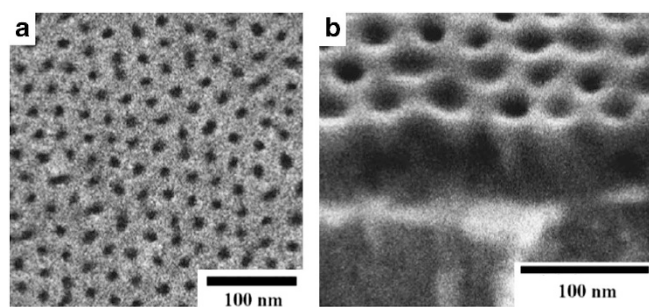


Figure 2 The (a) top view and (b) cross-sectional view FESEM micrographs of spin-coated PS-PLLA ($f_{\text{PLLA}}^{\text{V}}=0.26$) thin films on a silicon wafer from chlorobenzene at 50 °C after hydrolysis.³⁹

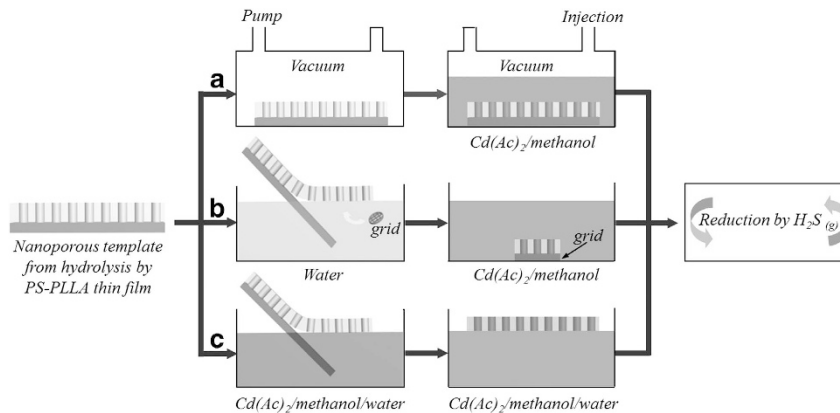


Figure 3 Schematic illustration of different pore-filling process.⁵⁴

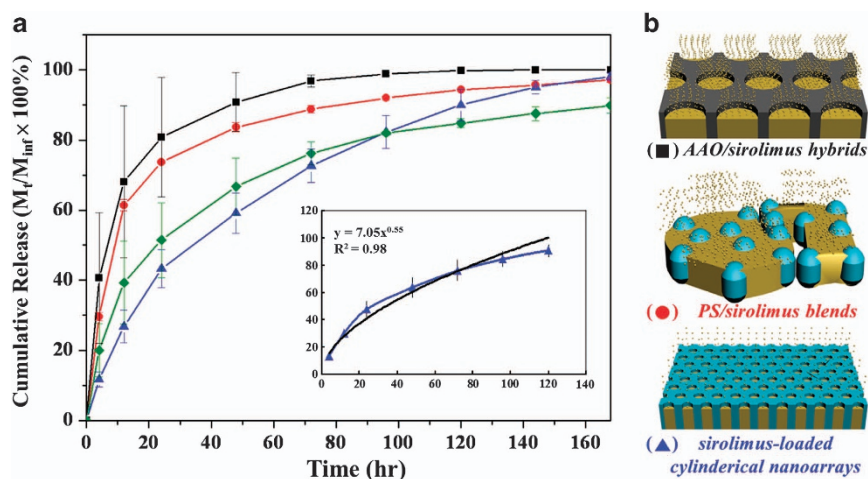


Figure 4 (a) Cumulative release profiles of sirolimus from sirolimus-loaded cylindrical nanoarrays (blue triangle), sirolimus-loaded lamellar nanoarrays (green diamond), AAO/sirolimus hybrids (black square), and PS/sirolimus blends (red circle). Inset plots the fitted curve (black line) for the release profile of the sirolimus-loaded cylindrical nanoarrays. M_{inf} is the infinite amount of loaded drugs in test templates; M_t is the cumulative amount of drug released at time t . (b) Schematic illustration of the sirolimus-loaded cylindrical nanoarrays, the AAO/sirolimus hybrids and the PS/sirolimus blends.⁵⁵

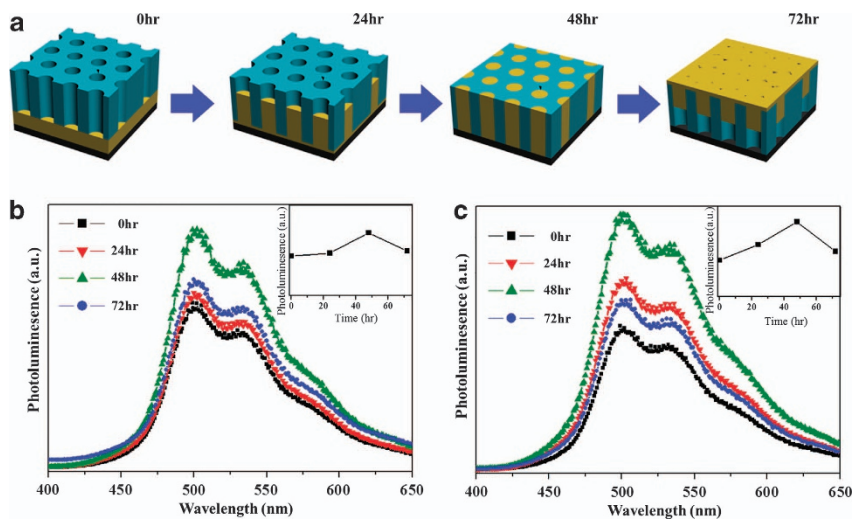


Figure 5 (a) Schematic illustration of the morphological evolution of pore-filling DP-PPV-PEO. Photoluminescence spectra of nanoporous PS templates on spin-coated (b) PPV3 and (c) PPV7 thin films for different solvent-annealing times. Insets show the plots of the intensity of first peak (498 nm) versus annealing time.⁵⁶

Templated electroplating

Electroplating is a plating process that uses electrical current to reduce the cations of a desired material from a solution and coat a conductive object with a thin layer of the material, such as metals or conjugated polymers.⁵⁷ Russell and co-workers⁵⁸ have successfully demonstrated the fabrication of Co-nanowires using nanoporous templates obtained from the self-assembly of BCP for electroplating. Subsequently, Russell and co-workers⁵⁹ used an electrophoretic process for the deposition of CdSe nanoparticles into cylindrical nanochannels in BCP films. Recently, we demonstrated a straightforward and effective method for fabricating double-length-scale patterned (that is, composite micro- and nano-patterned) carbon nanotube (CNT) arrays.⁴⁴ The formation of the composite patterns relies upon polymer, templating from the self-assembly of PS-PLLA on pre-patterned conducting substrates followed by the electroplating deposition of Ni. Therefore, a two-electrode field-emission device for patterned CNTs grown from PS-Ni composite films on micropatterned indium tin oxide (ITO) glass can be manufactured. Figures 6a–c present various FESEM images of the CNTs grown on the electroplated template of PS-PLLA formed on pre-patterned ITO glass. As shown in Figures 6a and b, CNTs can be selectively grown on the Ni sites over conducting sections, whereas no CNTs were observed on the non-conducting sections. Figure 6c shows the cross-sectional view of the CNTs grown on the conducting region. The average diameter of the nanotubes is ~ 45 nm and their distribution was quite narrow. In addition to the CNTs prepared from size-controlled Ni sites, the growth of CNTs with chemical vapor deposition (CVD) was also performed on a thin layer of Ni deposited by electroplating over the unpatterned ITO glass. To examine the performance of CNTs with double-length-scale patterned arrays, two-electrode field-emission devices for the patterned CNTs grown from PS/Ni composite films on micropatterned ITO glass were fabricated (Figure 6d). In addition, the growth of CNTs with CVD was also performed on a thin layer of Ni deposited by electroplating over the unpatterned ITO glass. As shown in Figure 6e, a significant improvement in the current density emission with a low threshold voltage and high emission efficiency can be observed in the double-length-scale patterned CNT arrays (hollow triangle) compared with the single-length-scale device (hollow circle).

Templated sol-gel reaction

The sol-gel process is a wet-chemical technique that is widely employed in materials science and ceramic engineering.

A considerable number of useful ceramic oxides, including the oxides of Al, Si, Ti, Zn and Zr, can be synthesized through the sol-gel process.^{60,61} Combining the sol-gel process with the templating of BCPs, various nanostructured ceramics can be fabricated after removal of the polymer template. The majority of studies focus on cylinder-forming BCP templates for fabricating low-dimensional nanostructures, such as nanodots and nanorods. For instance, Gutmann and co-workers⁶² demonstrated that hexagonally packed TiO₂ dots in a polymer matrix could be formed using polystyrene-*b*-poly(ethylene oxide) (PS-PEO) templates for one-step spin-coating from solutions with a TiO₂ precursor and PS-PEO, in which the precursor was selectively incorporated into the PEO micro-domain.^{61,62} In addition, the deposition of periodic TiO₂ nanorods, which were templated by a PS-P4VP BCP, was demonstrated by Shipp and co-workers.⁶³ The PS-P4VP thin films with P4VP cylinders orientated perpendicular to the substrate were used as BCP templates, and the sol-gel TiO₂ precursor can be captured in the P4VP microdomains. After oxygen plasma etching for degeneration of the polymer, TiO₂ nanorods with a regular arrangement can be generated.⁶³ Nevertheless, precisely fabricating three-dimensional, well-ordered, bicontinuous nanohybrid thin films remains challenging. Recently, we demonstrated the fabrication of a nanoporous gyroid ceramic with high porosity and well-defined three-dimensional nanostructures from PS-PLLA BCPs.⁴¹ Figures 7a–d show the formation of well-defined nanoporous gyroid SiO₂ from BCP templating. Nanoporous polymers with gyroid-forming nanochannels can be fabricated from the self-assembly of PS-PLLA followed by the hydrolysis of the PLLA blocks. Well-defined nanohybrids with SiO₂ gyroid nanostructures in a PS matrix can be obtained using nanoporous PS as a template for the templated sol-gel reaction. After removal of the PS matrix by UV treatment, the nanohybrids can be transferred to a highly porous inorganic gyroid network, as shown in Figure 7e. Because of the high porosity of the air voids and the low refractive index of the amorphous SiO₂ that is synthesized by the sol-gel process, nanoporous gyroid SiO₂ materials can be expected to possess extremely low refractive indices (as low as 1.10) (Figure 7f). Therefore, the nanoporous gyroid SiO₂ thin films can be utilized in appealing applications, such as anti-reflection structured materials that have high transmission, low reflection properties and superior environmental resistance. Furthermore, the low reflectivity of the nanoporous gyroid SiO₂ is evident over the complete spectral range of visible light, and it is nearly independent of the wavelength.

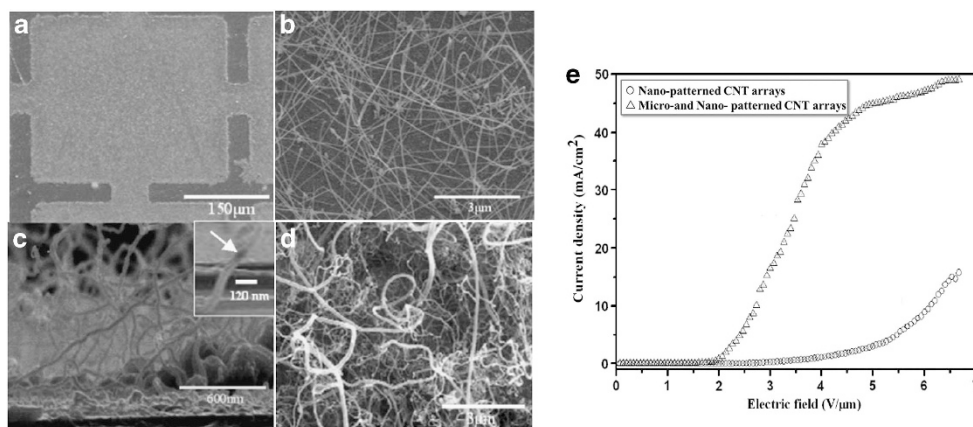


Figure 6 FESEM images of CNTs grown from PS-Ni composite films on micropatterned ITO glass: (a) low-magnification image; (b) high-magnification image; (c) cross-sectional image. (d) FESEM image of CNTs grown from a Ni layer deposited by electroplating on the substrate of nonpatterned ITO glass. (e) Field-emission current density versus the electric field for a two-electrode device of the CNTs grown from PS-Ni composite films on micropatterned ITO glass (hollow triangle) and nonpatterned ITO glass (hollow circle).⁴⁴

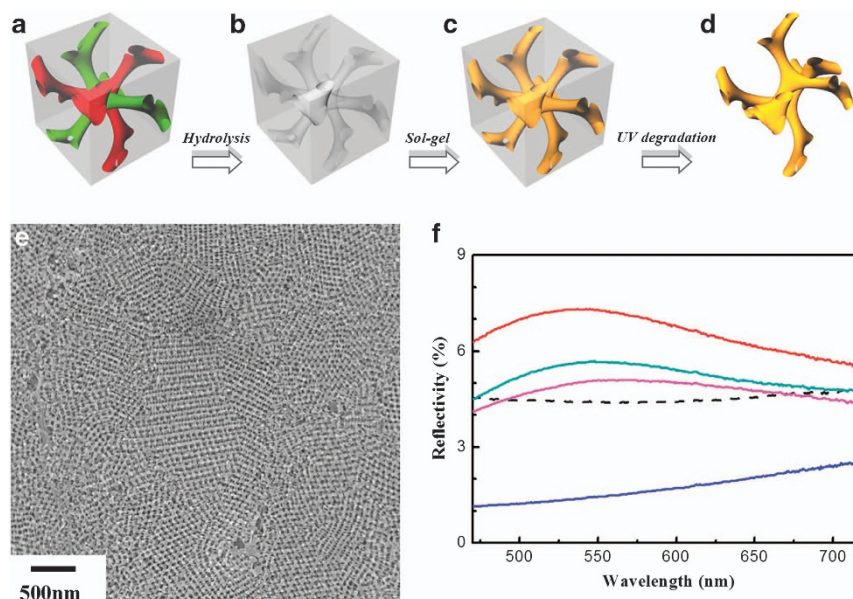


Figure 7 Schematic illustration for the creation of well-defined nanoporous gyroid SiO_2 from BCP templating: (a) PS-PLLA gyroid morphology (skeleton of double gyroid structure with two identical networks (green and red)); (b) Gyroid-forming nanoporous PS template after the removal of the minor PLLA network; (c) PS/ SiO_2 gyroid nanohybrids via the templated sol-gel process; (d) Nanoporous gyroid SiO_2 after the UV removal of the PS template. (e) FESEM micrograph of nanoporous gyroid SiO_2 from PS/ SiO_2 gyroid nanohybrids after the UV removal of the PS template. (f) Normal-incidence reflectances of quartz (black dashed line) and gyroid-forming nanostructures with different constituents: PS-PLLA BCP (solid red line); nanoporous PS template (solid purple line); PS/ SiO_2 gyroid nanohybrids (solid green line); and nanoporous gyroid SiO_2 (solid blue line) on a quartz substrate.⁴¹

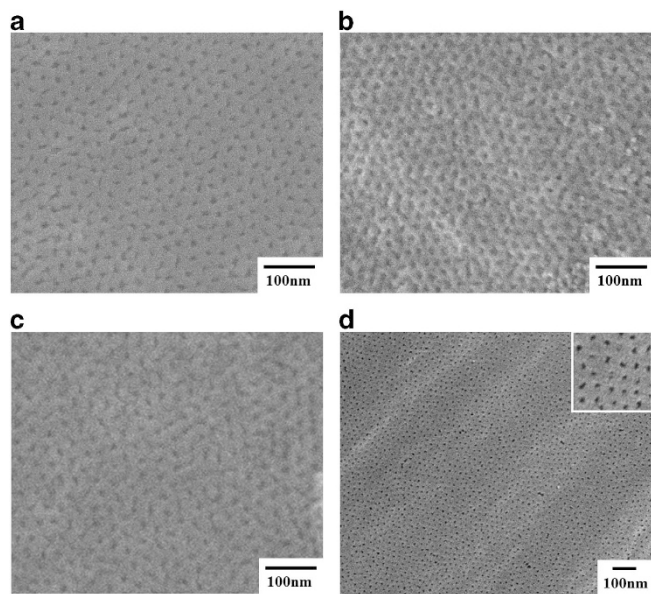


Figure 8 Top-view FESEM images of (a) PS, (b) PMMA and (c) PC topographic nanopatterns created using the silicon oxycarbide nanoporous mask for pattern transfer. (d) Top-view FESEM image of the mask after using the mask more than 30 times for pattern transfer; the inset shows the enlarged area.⁶⁷

SILICON-CONTAINING BCPS NANOPOROUS THIN FILM APPLICATIONS

Robust mask from silicon-containing BCP thin film

As mentioned above, the typical methods for generating nanoporous materials from the self-assembly of BCPs can be classified as wet and dry processes. The dry processes are usually conducted under vacuum

conditions, and the removable component will decompose under exposure to electrons or plasma ions without the use of any solvent. Recently, polymers composed of inorganic components (such as polydimethylsiloxane (PDMS)) have been extensively investigated because of their potential applications as etch-resistant materials for dry etching processes.⁵ The silicon-containing polymers can form a thin layer of silicon oxide under oxygen plasma treatment, which can resist further etching more than other types of polymers that only contain C, H, N and O atoms. Therefore, a number of studies on the synthesis of BCPs including blocks composed of silicon-containing polymer sequences for various applications have been demonstrated.^{6,63–65} For instance, Thomas and co-workers have demonstrated that PS-PDMS BCPs can be used as templates for the formation of silicon oxide nanoobjects in bulk with the use of oxygen plasma or exposure to UV light with ozone treatment.⁵ Ross and co-workers⁶ also investigated the graphoepitaxy method to guide the alignment of the cylinder phase PS-PDMS BCPs in confined volumes. Recently, we demonstrated that silicon-containing BCP thin films can also be used as etch-resistant masks for pattern transfer.⁶⁷ By using a one-step oxidation process in PS-PDMS thin films, the minor PS component can be easily etched into thru-pore nanochannels, while the PDMS matrix is simultaneously converted into a robust inorganic film. The patterned nanoporous inorganic film can be used as a robust mask for fabricating nanoporous polymeric thin films. As shown in Figure 8, the nanopatterns can be successfully transferred to PS, PMMA and PC with the features corresponding to the nanostructure of the nanoporous thin film. Moreover, no significant change with respect to the texture and size of the mask can be observed after using the mask for pattern transfer more than 30 times (Figure 8d).

Nanoring arrays from silicon-containing BCP thin films

Considering the geometries of nanostructures for potential applications, a ring-shaped nanostructure is useful in the design of devices

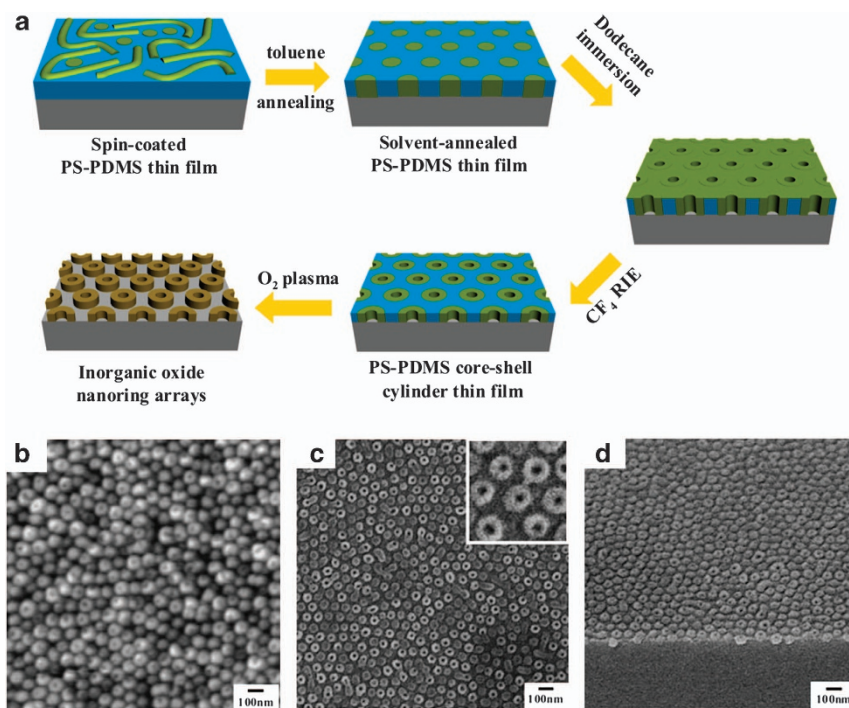


Figure 9 (a) Schematic illustration for the fabrication of silicon oxycarbide nanoring arrays from PS-PDMS thin films; (b) SPM height, (c) top-view FESEM, (d) cross-sectional view FESEM images of silicon oxycarbide nanoring arrays from oxidized PS-PDMS thin film (Inset shows the enlarged area).⁷²

such as sensors, transistors, optical and magnetic memories. Self-assembled BCPs nanostructures typically include dots, layers and pillars, but a ring-shaped nanostructure is not common. One way to create a ring-shaped nanostructure is to employ the self-assembly of triblock terpolymers for the formation of a core-shell cylinder thin film that contains low-aspect-ratio cylinders perpendicular to the substrate to use as a nanoring template.^{68,69} Ross and co-workers described the fabrication of nanoring arrays from PS-PDMS diblock copolymer thin films using topographical templates.⁷⁰ In addition, Russell and co-workers demonstrated that PS-PMMA BCPs can be used as templates to fabricate cobalt nanorings, which may provide single domain or vertex magnetic states at low fields.⁷¹ Consequently, using the unique features of nanorings as a mask for the patterning of magnetic thin films is appealing for data storage applications. In addition, the core-shell cylinder nanostructured thin films can be obtained from the self-assembly of PS-PDMS BCPs followed by a surface reconstruction process.⁷² Figure 9 presents an illustration of the fabrication of silicon oxycarbide nanoring arrays from the PS-PDMS BCPs. First, a spin-coated PS-PDMS with random orientation cylindrical PDMS nanostructures thin film is prepared. After a series of procedures including solvent annealing, dodecane immersion (surface reconstruction), CF_4 RIE and O_2 plasma, the core-shell cylinder PS-PDMS thin films can be obtained. On the basis of SPM observation, the height image of the core-shell cylinder thin film exhibits well-ordered nanoring arrays after oxygen plasma treatment (Figure 9b). To further examine the observed nanoring arrays, the oxidized sample was also examined by FESEM (Figure 9c). The inset of Figure 9c clearly demonstrates the features of the nanorings at high magnification. In addition, the cross-sectional view in the FESEM image of the oxidized thin film clearly shows the nanoring arrays with cylindrical nanochannels (Figure 9d). As estimated from the results of cross-sectional view in the FESEM images, the intrinsic aspect ratio of the nanorings is ~ 0.6 ; therefore, it is reasonable to suggest the

formation of nanorings (namely, low-aspect-ratio nano-objects). Therefore, this approach provides a simple route for creating core-shell cylinder nanostructured thin films that can be used as a template for fabricating inorganic oxide nanoring arrays.

CONCLUSIONS

Nanopatterning from the self-assembly of BCPs is very challenging and worthwhile, and many nanotechnological applications await such nanopatterned materials. BCPs have and will continue to attract the attention of scientists as self-assembling materials with nanoscopic features. External fields can direct BCP nanostructures into technologically desirable ordered patterns. Various methods were designed to display the successful control of PS-PLLA nanostructures in thin films. Here, both perpendicular cylindrical nanostructures and gyroid nanostructures aligned with the surface parallel to its (211) plane in PS-PLLA thin films can be achieved using solvent methods. There are many ways to exploit these attributes in applications; however, the formation of porosity has captured the imagination of many researchers. Owing to the degradable character of the PLLA component, the formation of topographic nanopatterns (nanoporous thin films) of PS-PLLA provides a simple path to prepare thin-film templates for templated synthesis to create functional nanohybrids. In addition, PS-PDMS can form inorganic nanoporous templates under oxygen plasma treatment. This nanoporous film could be used as an etch-resistant and reusable mask for pattern transfer into underlying polymeric substrates to directly generate nanoporous polymers. Furthermore, by taking advantage of the surface reconstruction approach, inorganic oxide nanoring arrays from PS-PDMS can be formed to be used for practical applications. Those nanoscale objects from the self-assembly of BCPs can be further arranged into well-defined configurations on a variety of predetermined substrates with one-dimensional, two-dimensional or three-dimensional arrangements to establish integrated systems. Moreover, the

nanoporous thin films have been exploited as templates to fabricate various nanostructured hybrids and nanocomposites in the past two decades, and exciting future advances in this field are yet to come.

- Bates, F. S. & Fredrickson, G. H. Block copolymer thermodynamics: theory and experiment. *Annu. Rev. Phys. Chem.* **41**, 525–557 (1990).
- Park, C., Yoon, J. & Thomas, E. L. Enabling nanotechnology with self-assembled block copolymer patterns. *Polymer* **44**, 6725–6760 (2003).
- Todd, E. M. & Hillmyer, M. A. *Porous Polymer from Self-Assembled Structures* (eds Silverstein, M. S., Cameron, N. R. & Hillmyer, M. A.) Ch. 2, 31–73 (John Wiley & Sons, New York, 2011).
- Zalusky, A. S., Olayo-Valles, R., Taylor, C. J. & Hillmyer, M. A. Mesoporous polystyrene monoliths. *J. Am. Chem. Soc.* **123**, 1519–1520 (2001).
- Chan, V. Z.-H., Thomas, E. L., Lee, V. L., Miller, R. D., Avgeropoulos, A. & Hadjichristidis, N. Periodic porous and relief nanostructure articles. US Patent Publication No. WO/00/02090.
- Jung, Y. S. & Ross, C. A. Orientation-controlled selfassembled nanolithography using a polystyrenepolydimethylsiloxane block copolymer. *Nano Lett.* **7**, 2046–2050 (2007).
- Kim, G. & Libera, M. Morphological development in solvent-cast polystyrene–polybutadiene–polystyrene (SBS) triblock copolymer thin films. *Macromolecules* **31**, 2569–2577 (1998).
- Fukunaga, K., Elbs, H., Magerle, R. & Krausch, G. Large-scale alignment of ABC block copolymer microdomains via solvent vapor treatment. *Macromolecules* **33**, 947–953 (2000).
- Temple, K., Kulbaba, K., Power-Billard, K. N., Manners, I., Leach, A., Xu, T., Russell, T. P. & Hawker, C. J. Spontaneous vertical ordering and pyrolytic formation of nanoscopic ceramic patterns from poly(styrene-*b*-ferrocenylsilane). *Adv. Mater.* **15**, 297–300 (2003).
- Albert, J. N. L., Young, W. S., Lewis, R. L., Bogart, T. D., Smith, J. R. & Epps, T. H. Systematic study on the effect of solvent removal rate on the morphology of solvent vapor annealed ABA triblock copolymer thin films. *ACS Nano* **6**, 459–466 (2012).
- Kim, S. H., Misner, M. J., Xu, T., Kimura, M. S. H. & Russell, T. P. Highly oriented and ordered arrays from block copolymers via solvent evaporation. *Adv. Mater.* **16**, 226–231 (2004).
- Park, S., Wang, J. Y., Kim, B., Chen, W. & Russell, T. P. Solvent-induced transition from micelles in solution to cylindrical microdomains in diblock copolymer thin films. *Macromolecules* **40**, 9059–9063 (2007).
- Park, S., Wang, J. Y., Kim, B., Xu, J. & Russell, T. P. A simple route to highly oriented and ordered nanoporous block copolymer templates. *ACS Nano* **2**, 766 (2008).
- Park, S., Kim, B., Xu, J., Hofmann, T., Ocko, B. M. & Russell, T. P. Lateral ordering of cylindrical microdomains under solvent vapor. *Macromolecules* **42**, 1278–1284 (2009).
- Lee, D. H., Park, S., Gu, W. Y. & Russell, T. P. Highly ordered nanoporous template from triblock copolymer. *ACS Nano* **5**, 1207–1214 (2011).
- Koppi, K. A., Tirrell, M. & Bates, F. S. Shear induced isotropic-to-lamellar transition. *Phys. Rev. Lett.* **70**, 1449 (1993).
- Chen, Z. R., Kornfield, J. A., Smith, S. D., Grothaus, J. T. & Satkowski, M. M. Pathways to macroscale order in nanostructured block copolymers. *Science* **277**, 1248–1253 (1997).
- Albalak, R. J., Thomas, E. L. & Capel, M. S. Thermal annealing of roll-cast triblock copolymer films. *Polymer* **38**, 3819–3825 (1997).
- Angelescu, D. E., Waller, J. H., Register, R. A. & Chaikin, P. M. Shear-induced alignment in thin films of spherical nanodomains. *Adv. Mater.* **17**, 1878–1881 (2005).
- Hong, Y. R., Adamson, D. H., Chaikin, P. M. & Register, R. A. Shear-induced sphere-to-cylinder transition in diblock copolymer thin films. *Soft Matter* **5**, 1687–1691 (2009).
- Morkved, T. L., Lu, M., Urbas, A. M., Ehrichs, E. E., Jaeger, H. M., Mansky, P. & Russell, T. P. Local control of microdomain orientation in diblock copolymer thin films with electric fields. *Science* **273**, 931–933 (1996).
- Thurn-Albrecht, T., Schotter, J., Kastle, G. A., Emley, N., Shibauchi, T., Krusin-Elbaum, L., Guarini, K., Black, C. T., Tuominen, M. T. & Russell, T. P. Ultrahigh-density nanowire arrays grown in self-assembled diblock copolymer templates. *Science* **290**, 2126–2129 (2000).
- Olszowka, V., Hund, M., Kuntermann, V., Scherdel, S., Tsarkova, L. & Boker, A. Electric field alignment of a block copolymer nanopattern: direct observation of the microscopic mechanism. *ACS Nano* **3**, 1091–1096 (2009).
- Hashimoto, T., Bodycomb, J., Funaki, Y. & Kimishima, K. The effect of temperature gradient on the microdomain orientation of diblock copolymers undergoing an order-disorder transition. *Macromolecules* **32**, 952–954 (1999).
- Mita, K., Takenaka, M., Hasegawa, H. & Hashimoto, T. Cylindrical domains of block copolymers developed via ordering under moving temperature gradient: real-space analysis. *Macromolecules* **41**, 8789–8799 (2008).
- De Rosa, C., Park, C., Thomas, E. L. & Lotz, B. Microdomain patterns from directional eutectic solidification and epitaxy. *Nature* **405**, 433–437 (2000).
- Ho, R. M., Hsieh, P. Y., Tseng, W. H., Lin, C. C., Huang, B. H. & Lotz, B. Crystallization-induced orientation for microstructures of poly(L-lactide)-*b*-poly(epsilon-caprolactone) diblock copolymers. *Macromolecules* **36**, 9085–9092 (2003).
- Tseng, W. H., Hsieh, P. Y., Ho, R. M., Huang, B. H., Lin, C. C. & Lotz, B. Oriented microstructures of polystyrene-*b*-poly(L-lactide) thin films induced by crystallizable solvents. *Macromolecules* **39**, 7071 (2006).
- Rockford, L., Liu, Y., Mansky, P., Russell, T. P., Yoon, M. & Mochrie, S. G. J. Polymers on nonperiodic, heterogeneous surfaces. *Phys. Rev. Lett.* **82**, 2602–2605 (1999).
- Kim, S. O., Solak, H. H., Stoykovich, M. P., Ferrier, N. J., de Pablo, J. J. & Nealey, P. F. Epitaxial self-assembly of block copolymers on lithographically defined nanopatterned substrates. *Nature* **424**, 411–414 (2003).
- Stoykovich, M. P., Muller, M., Kim, S. O., Solak, H. H., Edwards, E. W., de Pablo, J. J. & Nealey, P. F. Directed assembly of block copolymer blends into nonregular device-oriented structures. *Science* **308**, 1442 (2005).
- Ruiz, R., Kang, H. M., Detchervey, F. A., Dobisz, E., Kercher, D. S., Albrecht, T. R., de Pablo, J. J. & Nealey, P. F. Density multiplication and improved lithography by directed block copolymer assembly. *Science* **321**, 936–939 (2008).
- Ji, S. X., Nagpal, U., Liu, G. L., Delcambre, S. P., Muller, M., de Pablo, J. J. & Nealey, P. F. Directed assembly of non-equilibrium ABA triblock copolymer morphologies on nanopatterned substrates. *ACS Nano* **6**, 5440–5448 (2012).
- Segalman, R. A., Yokoyama, H. & Kramer, E. J. Graphoepitaxy of spherical domain block copolymer films. *Adv. Mater.* **13**, 1152–1155 (2001).
- Cheng, J. Y., Ross, C. A., Thomas, E., Smith, H. I. & Vancso, G. J. Fabrication of nanostructures with long-range order using block copolymer lithography. *Appl. Phys. Lett.* **81**, 3657–3659 (2002).
- Cheng, J. Y., Mayes, A. M. & Ross, C. A. Nanostructure engineering by templated self-assembly of block copolymers. *Nat. Mater.* **3**, 823–828 (2004).
- Park, S., Lee, D. H., Xu, J., Kim, B., Hong, S. W., Jeong, U., Xu, T. & Russell, T. P. Macroscopic 10-terabit-per-square-inch arrays from block copolymers with lateral order. *Science* **323**, 1030–1033 (2009).
- Tavakkoli, K. G. A., Gotrik, K. W., Hannon, A. F., Alexander-Katz, A., Ross, C. A. & Berggren, K. K. Templating three-dimensional self-assembled structures in bilayer block copolymer films. *Science* **1**, 1294–1298 (2012).
- Ho, R. M., Tseng, W. H., Fan, H. W., Chiang, Y. W., Lin, C. C., Ko, B. T. & Huang, B. H. Solvent-induced microdomain orientation in polystyrene-*b*-poly(L-lactide) diblock copolymer thin films for nanopatterning. *Polymer* **46**, 9362–9377 (2005).
- Elbs, H., Drummer, C., Abetz, V. & Krausch, G. Thin film morphologies of ABC triblock copolymers prepared from solution. *Macromolecules* **35**, 5570–5577 (2002).
- Hsueh, H. Y., Chen, H. Y., She, M. S., Chen, C. K., Ho, R. M., Gwo, S., Hasegawa, H. & Thomas, E. L. Inorganic gyroid with exceptionally low refractive index from block copolymer templating. *Nano Lett.* **10**, 4994–5000 (2010).
- Hsueh, H. Y. & Ho, R. M. Bicontinuous Ceramics with High Surface Area from Block copolymer templates. *Langmuir* **28**, 8518–8529 (2012).
- Ho, R. M., Chiang, Y. W., Tsai, C. C., Lin, C. C., Ko, B. T. & Huang, B. H. J. Three-dimensionally packed nano-helical phase in chiral block copolymers. *Am. Chem. Soc.* **126**, 2704–2705 (2004).
- Tseng, Y. T., Tseng, W. H., Lin, C. H. & Ho, R. M. Fabrication of double-length-scale patterns via lithography, block copolymer templating, and Electrodeposition. *Adv. Mater.* **19**, 3584–3588 (2007).
- Rzayev, J. & Hillmyer, M. A. Nanochannel array plastics with tailored surface chemistry. *J. Am. Chem. Soc.* **127**, 13373–13379 (2005).
- Park, M., Harrison, C., Chaikin, P. M., Register, R. A. & Adamson, D. H. Block copolymer lithography: Periodic arrays of similar to 10(11) holes in 1 square centimeter. *Science* **276**, 1401–1404 (1997).
- Chan, V. Z.-H., Hoffman, J., Lee, V. L., Iatrou, H., Avgeropoulos, A., Hadjichristidis, N., Miller, R. D. & Thomas, E. L. Ordered bicontinuous nanoporous and nanorelief ceramic films from self-assembling polymer precursors. *Science* **286**, 1716–1718 (1999).
- Urbas, A. M., Maldovan, M., DeRege, P. & Thomas, E. L. Bicontinuous cubic block copolymer photonic crystals. *Adv. Mater.* **14**, 1850–1853 (2002).
- Okumura, A., Nishikawa, Y. & Hashimoto, T. Nano-fabrication of double gyroid network structure via ozonolysis of matrix phase of polyisoprene in poly(2-vinylpyridine)-block-polyisoprene films. *Polymer* **47**, 7805–7812 (2006).
- Thurn-Albrecht, T., Steiner, R., DeRouchey, J., Stafford, C. M., Huang, E., Bal, M., Tuominen, M., Hawker, C. J. & Russell, T. P. Nanoscopic templates from oriented block copolymer films. *Adv. Mater.* **12**, 787–791 (2000).
- Jeong, U., Ryu, D. Y., Kim, J. K., Kim, D. H., Russell, T. P. & Hawker, C. J. Volume contractions induced by crosslinking: a novel route to nanoporous polymer films. *Adv. Mater.* **15**, 1247–1250 (2003).
- Bang, J., Kim, S. H., Drockenmuller, E., Misner, M. J., Russell, T. P. & Hawker, C. J. Defect-free nanoporous thin films from ABC triblock copolymers. *J. Am. Chem. Soc.* **128**, 7622–7629 (2006).
- Lin, Z., Kim, D. H., Wu, X. D., Boosahda, L., Stone, D., LaRose, L. & Russell, T. P. A rapid route to arrays of nanostructures in thin films. *Adv. Mater.* **14**, 1373–1376 (2002).
- Lo, K. H., Tseng, W. H. & Ho, R. M. In-situ formation of CdS nanoarrays by pore-filling nanoporous templates from degradable block copolymers. *Macromolecules* **40**, 2621–2624 (2007).
- Lo, K. H., Chen, M. C., Ho, R. M. & Sung, H. W. Pore-filling nanoporous templates from degradable block copolymers for nanoscale drug delivery. *ACS Nano* **3**, 2660–2666 (2009).
- Lo, K. H., Ho, R. M., Liao, Y. M., Hsu, C. S., Massuyeau, F., Zhao, Y. C., Lefrant, S. & Duvaill, J. L. Induced chain alignment of conjugated polymers within nanoporous template. *Adv. Funct. Mater.* **21**, 2729–2736 (2011).
- Whitney, T. M., Jiang, J. S., Searson, P. C. & Chien, C. L. Fabrication and magnetic properties of arrays of metallic nanowires. *Science* **261**, 1316–1319 (1993).

- 58 Thurn-Albrecht, T., Schotter, J., Kastle, C. A., Emley, N., Shibauchi, T., Krusin-Elbaum, L., Guarini, K., Black, C. T., Tuominen, M. T. & Russell, T. P. Ultrahigh-density nanowire arrays grown in self-assembled diblock copolymer templates. *Science* **290**, 2126–2129 (2000).
- 59 Zhang, Q., Xu, T., Butterfield, D., Misner, M. J., Ryu, D. Y., Emrick, T. & Russell, T. P. Controlled placement of CdSe nanoparticles in diblock copolymer templates by electrophoretic deposition. *Nano Lett.* **5**, 357–361 (2005).
- 60 Pierre, A. C. *Introduction to sol-gel processing* (Kluwer Academic, Boston, 1998).
- 61 Hench, L. L. & West, J. K. The sol-gel process. *Chem. Rev.* **90**, 33–72 (1990).
- 62 Kim, D. H., Sun, Z. C., Russell, T. P., Knoll, W. & Gutmann, J. S. Organic-inorganic nano-hybridization by block copolymer thin films. *Adv. Funct. Mater.* **15**, 1160–1164 (2005).
- 63 Chinthamanipeta, P. S., Lou, Q. & Shipp, D. A. Periodic titania nanostructures using block copolymer templates. *ACS Nano* **5**, 450–456 (2011).
- 64 Li, L. & Yokoyama, H. Nanoscale silica capsules ordered on a substrate: Oxidation of nanocellular thin films of poly(styrene-*b*-dimethylsiloxane). *Angew. Chem. Int. Ed.* **45**, 6338–6341 (2006).
- 65 Rider, D. A., Cavicchi, K. A., Vanderark, L., Russell, T. P. & Manners, I. Orientationally controlled nanoporous cylindrical domains in polystyrene-*b*-poly(ferrocenylethylmethylsilane) block copolymer films. *Macromolecules* **40**, 3790–3796 (2007).
- 66 Bitá, I., Yang, J. K. W., Jung, Y. S., Ross, C. A., Thomas, E. L. & Berggren, K. K. Graphoepitaxy of self-assembled block copolymers on two-dimensional periodic patterned templates. *Science* **321**, 939–943 (2008).
- 67 Chao, C. C., Wang, T. Z., Ho, R. M., Georgopoulos, P., Ageropoulos, A. & Thomas, E. L. Robust block copolymer mask for nanopatterning polymer films. *ACS Nano* **4**, 2088–2094 (2010).
- 68 Guo, S. W., Rzaev, J., Bailey, T. S., Zalusky, A. S., Olayo-Valles, R. & Hillmyer, M. A. Nanopore and nanobushings Arrays from ABC triblock thin films containing two etchable blocks. *Chem. Mater.* **18**, 1719–1721 (2006).
- 69 Park, S., Wang, J. Y., Kim, B. & Russell, T. P. From nanorings to nanodots by patterning with block copolymers. *Nano Lett.* **8**, 1667–1672 (2008).
- 70 Jung, Y. S., Jung, W. & Ross, C. A. Nanofabricated concentric ring structures by templated self-assembly of a diblock copolymer. *Nano Lett.* **7**, 2975–2981 (2008).
- 71 Singh, D. K., Krotkov, R. V., Xiang, H. Q., Xu, T. & Russell, T. P. Arrays of ultrasmall metal rings. *Nanotechnology* **19**, 245305 (2008).
- 72 Chao, C. C., Ho, R. M., Georgopoulos, P., Ageropoulos, A. & Thomas, E. L. Silicon oxy carbide nanorings from polystyrene-*b*-polydimethylsiloxane diblock copolymer thin films. *Soft Matter* **6**, 3582–3587 (2010).



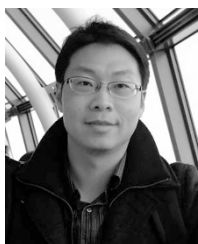
This work is licensed under a Creative Commons Attribution-NonCommercial-NoDerivs 3.0 Unported License. To view a copy of this license, visit <http://creativecommons.org/licenses/by-nc-nd/3.0/>



Mr Ming-Shiuan She received his MS degree from the Department of Chemical Engineering, National Tsing Hu University (Taiwan) in 2008 under the supervision of Professor Rong-Ming Ho. After graduation, he continued to study in the group of Professor Rong-Ming Ho, and currently he is a PhD candidate. His research interests include self-assembled materials, nanopatterning technology and nanofabrication. His current research focuses on the templated self-assembling processes for the formation of ordered and oriented nanostructures in block copolymers.



Mr Ting-Ya Lo received his MS degree from the Department of Chemical Engineering, National Tsing Hu University (Taiwan) in 2011 under the supervision of Professor Rong-Ming Ho. After graduation, he continued to study in the group of Professor Rong-Ming Ho, and currently he is a PhD candidate. His research interests include block copolymer physics, nanopatterning technology, three-dimensional electron tomography and templated self-assembling process. His current research focuses on the self-assembled morphologies of silicon-containing block copolymer from solution casting or in solution state, and also the orientation control of nanostructured thin films from block copolymers.



Dr Han-Yu Hsueh received his bachelor's degree from the Department of Chemical Engineering, National Tsing Hua University (Taiwan) in 2005. Afterward he moved to Department of Material Science and Engineering, National Taiwan University (Taiwan) for graduate study under the supervision of Professor Wen-Bin Liao and received MS degree in 2007. In 2011, he received his PhD in Chemical Engineering from National Tsing Hua University (Taiwan), working with Professor Rong-Ming Ho, and now he is a Post-doctoral Fellowship in the laboratory of Professor Ho. The title of his PhD thesis is 'Nanohybrid and Nanoporous Materials from Chiral Block Copolymer Templating'. His current researches focus on the fabrication of various nanohybrids and nanoporous materials based on the templating of block copolymers for applications.



Professor Rong-Ming Ho received his PhD degree from the Institute of Polymer Science, University of Akron (USA) in 1995 under the supervision of Professor Stephen ZD Cheng. He then moved to Minneapolis and worked as a post-doctoral fellow in the Department of Chemical Engineering and Materials Science, University of Minnesota (USA) with Professors Christopher W Macosko and Frank S Bates. In 1997, he returned to Taiwan and took a faculty position in the Department of Chemical and Engineering, National Chung Hsing University (Taiwan) as an assistant professor. In 2002, he transferred to the Department of Chemical Engineering, National Tsing Hua University (Taiwan) as an associate professor. In 2006, he was promoted to the rank of full professor. He was appointed as distinguished professor in 2009. His current researches focus on nanomaterials from self-assembly of block copolymers and supramolecules, nanopatterning technologies through integration of top-down and bottom-up methods and inorganic/organic hybridization from templating of block copolymers. He received the Outstanding Research Award of Taiwan in 2006.